

14 **Abstract**

15 African cultivated rice, *Oryza glaberrima*, is characterized by its glabrous glumes.
16 During domestication, the pubescent glumes of its wild ancestor, *Oryza barthii*, lost
17 their trichomes, and in this study, we show that *GLABROUS GLUME 5 (GLAG5)*, a
18 *WUSCHEL*-like homeobox transcription factor on chromosome 5, is required for
19 trichome development. DNA methylation associated with an *hAT* transposable
20 element inserted in the promoter region of *GLAG5* was found to reduce its expression,
21 leading to the formation of glabrous glumes and leaves in African cultivated rice.
22 Among 82 African cultivated rice varieties investigated in this study, 59
23 (approximately 71%) lines exhibited glabrous glumes and harbored the *hAT*
24 transposon; however, the other 23 varieties, which exhibit pubescent glumes
25 (approximately 29%), lacked the *hAT* transposon, indicating that *glag5* had undergone
26 strong artificial selection. The π_w/π_c ratios also showed the *hAT* transposon insertions
27 influenced the genetic diversity of an approximately 150-kb interval encompassing
28 the *GLAG5* locus. The identification of the *GLAG5* gene provides new insights into
29 the domestication of cultivated rice in Africa. We speculate that the selection of
30 varieties with mutations in their promoter regions is an important aspect of crop
31 domestication.

32

33 **Introduction**

34 African cultivated rice (*Oryza glaberrima*) was domesticated from its wild
35 progenitor *Oryza barthii* in Africa more than 3000 years ago (Purugganan, 2014).
36 During domestication, farmers selected for morphological traits that facilitated
37 cultivation and harvesting, which included reduced seed shattering, erect plant
38 architecture and short-awn or awnless seeds. African rice is a valuable genetic
39 resource containing resistance genes to biotic and abiotic stresses, such as Rice
40 Yellow Mottle Virus, high temperature, soil acidity, iron toxicity and drought (Linares,
41 2002; Thiemele et al 2010; Jones et al., 2013; Wambugu et al., 2013; Li et al., 2015).
42 Owing to its genetic importance, the origin and evolution of African rice has been
43 studied extensively over several decades (Ammiraju et al., 2008; Van Andel, 2010;
44 Molina et al., 2011; Sakai et al., 2011; Chen et al., 2013; Stein et al., 2018). Recent
45 studies have identified the genes controlling the reduction of seed shattering and erect
46 plant architecture characteristics in African cultivated rice (Wu et al., 2017; Hu et al.,
47 2018; Lv et al., 2018), and this information has provided new insights into its
48 domestication.

49 *Oryza glaberrima* is known as glabrous rice, and it is characterized by glabrous
50 glumes and leaves. However, African wild rice is typically densely covered by hard
51 (thorn-like) trichomes on the seeds and soft trichomes on the leaves, which aid seed
52 dispersal and provide protection against seed predation by birds and other animals.
53 The glabrous glumes of *O. glaberrima* are valued for hand-harvesting, because they
54 decrease skin irritation during threshing, drying and milling, and reduce the amount of
55 storage space required (Lim et al., 1984). The loss of trichomes is considered to be an
56 important event during the domestication of wild rice. However, the molecular genetic
57 mechanisms involved in the loss of trichomes remain largely unknown.

58 Transposable elements (TEs), or fragments of DNA that can move from one
59 location in the genome to another, are major components of eukaryotic genomes
60 (Feschotte et al., 2002). In rice, over 35% of the genomic content is composed of TEs,
61 and generic sequences are embedded in these vast expanses of TEs (Ma et al., 2020).
62 TEs can influence nearby gene expression either through *cis*-acting elements residing

63 in their own sequences or by changing the DNA or chromatin methylation states of
64 adjacent genes (Studer et al., 2011; Friedli and Trono, 2015; Li et al., 2017; Peng et
65 al., 2019). To maintain genomic stability, TEs are usually silenced and inactive,
66 owing to DNA and chromatin modifications.

67 In this study, we describe the isolation and characterization of *GLABROUS*
68 *GLUME 5* (*GLAG5*), which controls the formation of glabrous glumes and leaves in
69 African rice. This gene was found to encode a homeobox domain transcription factor
70 located on chromosome 5. Furthermore, we show that an *hAT* transposon insertion in
71 the *GLAG5* promoter during African cultivated rice domestication may have repressed
72 gene expression through DNA methylation and led to the development of glabrous
73 glumes.

74

75 **Results**

76 **Comparison of plant phenotypes between W1411 and IRGC104165**

77 The seeds of African wild rice (*O. barthii*) are densely covered by hard
78 (thorn-like) trichomes that are macroscopic and sharp, whereas the hulls of African
79 cultivated rice are glabrous and smooth (Fig. 1A and 1B). The hard trichomes of the
80 wild rice cause the seeds to stick to clothes and penetrate skin, causing inflammation,
81 while soft trichomes cover the adaxial surface of the leaves (Fig. S1), which can cause
82 skin irritation. The hard trichomes are critical for efficient propagation and
83 dissemination of wild rice seeds under natural conditions, serving to protect them
84 from predation and aid dispersal (Fig. S2). However, trichomes decrease the
85 efficiency of grain packaging, while the glabrous glumes of cultivated rice facilitate
86 harvesting and storage (Fig. S3). To further investigate the differences in the hulls and
87 leaves between African wild and cultivated rice, the leaf and grain phenotypes of the
88 African wild rice line W1411 (IRGC100119) and the African cultivated cultivar
89 IRGC104165 were examined using stereomicroscopy and scanning electron
90 microscopy (SEM). Epidermal cells on surface of glumes from wild rice were seen to
91 bulge (Fig. 1C). However, no swollen epidermal cells were found on surface of the

92 glumes from the cultivated rice (Fig. 1D). The swollen epidermal cells formed
93 basipetally along the glume, and they elongated and sharpened upwardly to form hard
94 (thorn-like) trichomes at the late stage in W1411 (Fig. 1E). However, no barbs formed
95 at any time during glume development in the cultivated rice, resulting in glabrous
96 glumes (Fig. 1F).

97 **Map-based cloning of *GLAG5***

98 To isolate the gene controlling the transition from the barbed hulls of wild rice to
99 the glabrous glumes of cultivated rice, we carried out a genetic analysis using an F₂
100 population containing 182 individuals developed from a cross between the African
101 wild rice cultivar W1411 (IRGC100119) and the African cultivated cultivar rice line
102 IRGC104165. Among the 182 individuals, 138 exhibited barbed glumes and 48
103 revealed smooth glumes. A 3:1 ($X^2 = 0.0645$, $P > 0.05$) segregation ratio was
104 determined, indicating the glabrous glume phenotype was controlled by a single
105 recessive gene, designated as *GLAG5*, which was mapped between SSR markers C03
106 and RM593 on the short arm of chromosome 5.

107 Using 4500 recessive homozygotes with the glabrous hull phenotype from the F₂
108 population and 6 newly developed markers, we ultimately delimited *GLAG5* to a
109 15.9-kb region between the C06 and C02 markers. This region contained only one
110 predicted gene, *OBART05G01300*, in the African wild rice reference genome
111 (https://ensembl.gramene.org/Oryza_barthii/Info/Index). No difference was found in
112 the coding region of *OBART05G01300* between the wild (W1411) and cultivated
113 (IRGC104165) rice. However, a transposon (478 bp) was found to lie in the promoter
114 region of this gene in the IRGC104165 genome (Figs. 2A, 2B, S4). These results
115 suggested that *OBART05G01300* is the *GLAG5* gene controlling trichome
116 development in the hulls of African rice species.

117 To confirm this hypothesis, we generated a construct (p*GLAG5*) by placing a
118 4.04-kb genomic fragment from wild rice (W1411), covering the *OBART05G01300*
119 gene only, into the vector pCAMBIA1300. Owing to the recalcitrance of the
120 cultivated line IRGC104165 to regenerating shoots from calli, we introduced the
121 p*GLAG5* construct into another African cultivated rice cultivar (WK21) which also

122 has glabrous glumes. The 11 independent transgenic lines all grew trichomes on their
123 glumes (Fig. 2C–2F) and demonstrated small bulges on their leaves (Fig. 2G and 2H).
124 These results confirmed that the *OBART05G01300* gene was indeed *GLAG5*.

125 **Subcellular localization and functional analysis of *GLAG5***

126 The *GLAG5* protein was predicted to encode a transcription factor and contains a
127 nuclear localization signal. Further analyses revealed that *GLAG5* contains a
128 homeodomain (HD), which is a DNA-binding domain and a *WUSCHEL* domain,
129 indicating that it belongs to the *WUSCHEL*-like homeobox (WOX) family. The
130 *GLAG5*-green fluorescent protein fusion protein specifically localized to the nuclei in
131 rice protoplast cells (Fig. S5). These results indicated that *GLAG5* encodes a
132 transcription factor.

133 To further validate the function of *GLAG5*, we knocked out the endogenous
134 *OBART05G01300* gene in W1411 using CRISPR-Cas9 genome editing technology.
135 Using PCR and sequencing analysis, we obtained five heterozygous transgenic plants
136 in the T0 generation by PCR and sequencing analyses. These five transgenic plants
137 were self-pollinated to generate T1 generations and genotyped using the primers
138 flanking the target region. Different knockout lines with homozygous mutations
139 showed the same phenotype and all exhibited glabrous glumes and leaves (Fig. 3A–
140 3F). These results further indicated that the *OBART05G01300* is *GLAG5*.

141 Interestingly, the homozygous mutations also exhibited other phenotypes. The
142 auricles and ligules of wild rice W1411 carried trichomes, while the auricles of
143 CAS9-*GLAG5* was disappeared (Fig. 3G and 3H). Moreover no trichomes appeared
144 on the ligules of the homozygous mutants (Fig. S6H and S6I). In addition, the glumes
145 of CAS9-*GLAG5* were malformed and accompanied by sterile, short and smooth
146 awns (Fig. 3I, 3J, S6A–S6G). Compared with W1411, the CAS9-*GLAG5* plants were
147 dwarfed (Fig. 3K).

148

149 **A transposon in the promoter of *GLAG5* led to glabrous glumes in *O. glaberrima***

150 To identify the mutation responsible for glabrous glumes, we analyzed the 478
151 bp inserted into the promoter of *GLAG5* that lay 139 bp upstream of the translation

152 initiation site. On the basis of the TE classification characteristics, there was an 8-bp
153 target-site duplication and 23-bp terminal inverted repeat in the 478-bp insertion. We
154 identified the insertion to be an *hAT* transposon, which is a Class II transposon (Fig.
155 4A).

156 Gene expression is usually repressed by the TE insertion into a promoter. To
157 determine the effects of the *hAT* transposon on gene expression, we examined the
158 expression pattern of *GLAG5* using quantitative RT-PCR (qRT-PCR). The TE reduced
159 the expression of *GLAG5* in the leaves, leaf sheaths, and young panicles (Fig. 4B).
160 Moreover, GUS activity in transgenic plants expressing the β -glucuronidase reporter
161 gene fused to a *GLAG5* promoter fragment was detected in the young panicles, ligules
162 and leaves (Fig. S7A–S7D).

163 To further validate the influence of the *hAT* TE, we independently cloned the
164 W1411 and IRGC104165 sequences that differed into reporter constructs upstream of
165 the promoter of the cauliflower mosaic virus, the firefly luciferase (LUC) ORF and
166 the nopaline synthase terminator and compared their effects on gene expression in rice
167 protoplasts. The rice construct containing the *hAT* TE significantly repressed LUC
168 activity relative to the W1411 construct without the *hAT* TE (Fig. 4C).

169 In general, a TE insertion induces epigenetic modifications of either DNA or
170 histones. To clarify the molecular mechanisms behind the promoter-associated
171 inhibitory activity of *GLAG5*, the sequence around the *hAT* TE insertion region was
172 analyzed using <http://www.urogene.org/methprimer/>. Two CpG islands in the *hAT* TE
173 insertion region were identified (Fig. S7E). Then, the methylation status of the CpG
174 sites within the two CpG islands was detected using methylation-specific PCR. As
175 shown in Fig. 4D, the *hAT* TE insertion caused DNA methylation of IRGC104165.

176 In summary, the *hAT* TE insertion caused DNA methylation that reduced the
177 expression of *GLAG5*, resulting in glabrous glumes.

178 **Evidence of positive selection on the *GLAG5* region in *O. glaberrima***

179 To further determine whether other glabrous African cultivated rice lines are the
180 result of TE insertions, we genotyped this locus in 12 diverse wild and 82 cultivated
181 rice accessions. Interestingly, none of the investigated wild rice accessions carried the

182 *hAT* TE, indicating that the TE insertion is most likely a *de novo* mutation that
183 occurred following early domestication (Table S1). Among the 82 cultivated rice
184 varieties, the 58 varieties (approximately 71%) exhibiting glabrous glumes harbored
185 the *hAT* TE; however, the other 24 varieties (approximately 29%) without glabrous
186 glumes lacked the *hAT* TE (Fig. 5A and 5B). These results suggested that the *hAT* TE
187 insertion in the promoter of *GLAG5* was under strong positive selection during the
188 domestication of African cultivated rice.

189 Selective signatures from domestication include a reduction in nucleotide
190 diversity and altered allele frequencies of the domestication-associated loci (Xu et al.,
191 2011). A favorable mutant allele greatly affects the genetic diversity at the selected
192 gene locus, and it has a strong impact on its surrounding genome regions. To
193 determine the genomic regions resulting from the artificial selection of *glag5* in *O.*
194 *glaberrima*, we examined and compared the nucleotide diversity (π) within the
195 regions around *GLAG5* between wild and cultivated rice. As shown in Fig. 5C, an
196 approximate 150-kb interval encompassing the *GLAG5* locus was influenced by the
197 *hAT* TE during domestication.

198

199 **Discussion**

200 Crop domestication is a progress of genetically modifying a wild species to meet
201 human needs (Doebley et al., 2006). The identification of key genes controlling
202 domestication-related traits helps to reveal crop origins. The African cultivated rice *O.*
203 *glaberrima* was independently domesticated from its wild progenitor *O. barthii* in
204 Africa more than 3000 years ago. Genes reducing seed shattering and leading to erect
205 plant architecture have been identified previously in African cultivated rice (Wu et al.,
206 2017; Hu et al., 2018; Lv et al., 2018), and they provide insights into the
207 domestication process.

208 *Oryza glaberrima* is characterized by its glabrous glumes. In this study, we
209 identified the *GLAG5* gene, which controls trichome development in African wild rice,
210 and found a *hAT* TE lying in the promoter region of the *GLAG5* gene. The TE reduced

211 *GLAG5* expression levels in the glumes and leaves, which consequently resulted in
212 their glabrous phenotypes in African cultivated rice. In addition to Africa, glabrous
213 rice is cultivated in the USA and on the Yunnan-Guizhou Plateau in China. In a
214 previous study, Angeles-Shim et al. (2012) found a few SNPs in the CDs between *O.*
215 *glaberrima* (IRGC104038) and *Oryza sativa* Koshihikari, which resulted in three
216 amino acid substitutions and a serine deletion. However, the sequence analysis
217 showed that both glabrous and pubescent lines of *O. glaberrima* carry the same amino
218 acid substitutions and deletion relative to Koshihikari, which implied that the changes
219 in the CDs did not cause the glabrous glumes. However, the expression of *GLAG5* in
220 glabrous cultivars was lower than in pubescent cultivars and no sequence differences
221 were found in the 2-kb promoter regions of *O. glaberrima* and Koshihikari.

222 In the present study, the 2.5-kb sequence in the promoter region of *GLAG5* was
223 compared between W14111 and IRGC104165. There was a 478-bp insertion (the *hAT*
224 TE) in the *O. glaberrima* promoter region (Fig. S4). Among the 82 African cultivated
225 rice varieties used in our research, the 59 (approximately 71%) varieties exhibiting
226 glabrous glumes harbored the *hAT* TE; however, the other 23 lines exhibiting
227 pubescent glumes (approximately 29%) lacked the *hAT* TE. The result indicated that
228 the *hAT* TE insertion in the promoter of *GLAG5* led to glabrous glumes in African
229 cultivated rice (Table S1). Two previous studies (Li et al., 2012; Zhang et al., 2012)
230 showed that glabrous glumes and leaves are controlled by a reduction in *NUDA/GL-1*
231 expression in Asian rice; however, no mutations in these CDs or promoters were
232 found between the glabrous and pubescent cultivars of *O. sativa*. Thus, the results
233 indicated that the glabrous glumes in Asian rice (*O. sativa*) and African rice (*O.*
234 *glaberrima*) are of independent origin, resulting from different mutations.

235 In many tissues, HD-leucine zippers (HD-Zip) plays important roles during
236 trichome initiation in the epidermis. In *Arabidopsis*, *GL2* is an HD transcription factor
237 that promotes trichome initiation in shoots and mucilage biosynthesis in seeds, but
238 inhibits root-hair formation in roots (Chen and Wang, 2019). In tomato, the HD-Zip
239 transcription factor *Woolly* plays crucial roles in trichome formation and embryo
240 development (Yang et al., 2011). An HD-Zip gene, *Tri*, is involved in multicellular

241 trichome initiation in cucumber (Wang et al., 2016). *GLAG5* contains an HD and a
242 *WUSCHEL* domain, which indicated that it belonged to the *WOX* gene family.
243 *GLAG5* also plays an important role in trichome initiation. In Asian rice, *OsWOX3B* is
244 an essential regulator of trichome initiation, and auxin-related genes are regulated by
245 *OsWOX3B*. Moreover, *HL6* induces the expression of several auxin-related genes that
246 determine trichome elongation, and this induction may be enhanced by *OsWOX3B*
247 interacting with *HL6* (Sun et al., 2017). *GLAG5* and *OsWOX3B* are homologous
248 genes, and, therefore, trichome development in African wild rice may also involve
249 *OsWOX3B*.

250 The *WOX* gene family also plays important roles in regulating the development
251 of plant tissues and organs (Zhang et al., 2010). Interestingly, loss-of-function
252 mutations of *GLAG5* not only cause glabrous glumes and leaves, but also result in
253 auricle disappearance, glabrous ligules, glume malformation, sterility, short and
254 smooth awns and dwarfing (Fig. 3G–3K). Thus, *GLAG5* has pleiotropic effects with
255 regard to glumes and sterility, which are necessary for the normal growth of rice.
256 Either intentionally or fortuitously, ancient humans in West Africa selected for rice
257 that have a TE insertion in the promoter region rather than a change in the gene
258 coding region. The presence of the TE through the DNA methylation of *GLAG5*
259 reduced its expression in the glumes and leaves, leading to glabrous glumes, while
260 maintaining normal spikelets and plant architecture.

261 A CACTA-like TE within the maize *ZmCCT10* promoter and a Harbinger-like
262 TE within the *ZmCCT9* promoter were strongly selected to facilitate the adaptation of
263 maize to higher latitudes after its domestication (Yang et al., 2013; Huang et al.,
264 2018). A TE insertion into the maize domestication gene *tb1* leads to an increase in
265 apical dominance compared with its wild ancestor, teosinte, by increasing gene
266 expression (Studer et al., 2011). A MITE insertion represses *ZmNAC111* expression
267 through the DNA and histone methylation of its nearby regions, and this is
268 significantly associated with natural variations in maize drought tolerance (Mao et al.,
269 2015). Thus, TE insertions into promoter regions can finely regulate gene expression
270 and selection for the mutated gene promoter is an important aspect of crop

271 domestication.

272

273 **Materials and Methods**

274 **Plant materials and growth conditions**

275 To clone of *GLAG5*, W1411 and IRGC104165 plants were used. W1411, an African
276 wild rice accession (*O. barthii*), was collected from Sierra Leone. IRGC104165, a
277 cultivar of African rice (*O. glaberrima*), was collected from Guinea. The F₂
278 segregating population was derived from the cross between W1411 and IRGC104165.
279 For the genetic transformation experimentat, we used an accession of IRGC104038
280 (*O. glaberrima*), WK21. Details of the 82 *O. glaberrima* accessions and 12 *O. barthii*
281 accessions are listed in Table S1. All plants were grown under field conditions in
282 Beijing or Sanya, Hainan Province, China.

283

284 **Phenotype observations**

285 Leaves and auricles were dissected, fixed overnight at 4°C in 1:1:18 formalin:glacial
286 acetic:70% ethanol and dehydrated in a graded ethanol series (50%, 70%, 80%, 90%,
287 95% and 100%). Samples were critical-point-dried, mounted, gold plated, observed
288 and photographed using a Hitachi S-2460 scanning electron microscope.

289

290 **Vector construction**

291 The complementary vector was generated by placing a 4.044-kb genomic fragment
292 from W1411, which contained the entire *GLAG5* ORF (0.841 kb), the promoter
293 region (2.506 kb) and the 3' -untranslated region (0.697 kb), into pCAMBIA1300.
294 The complementary vector was transformed into WK21. The genome-editing vector
295 of *GLAG5* was generated using the target 'tgctggaggagatgtacag'. The genome-editing
296 vectors was transformed into W1411. To construct the *GLAG5* promoter:GUS fusion
297 plasmid, an approximately 2-kb DNA fragment comprising the promoter sequence of
298 *GLAG5* in W1411 was amplified and cloned into the pCAMBIA1301-GUS-nos
299 vector. The pCAMBIA1301-GUS-nos vector was transformed into ZH17.

300

301 **RNA extraction and qRT-PCR.**

302 Total RNA was extracted using TRIzol reagent (Invitrogen) and purified using an
303 RNeasy Plant Mini Kit (QIAGEN) following the manufacturer's instructions.
304 First-strand cDNA synthesis was carried out using a BcaBEST RNA PCR Kit
305 (TaKaRa). The qRT-PCR was performed using the first-strand cDNA as the template.
306 Endogenous ubiquitin transcripts were used to normalize the expression levels. The
307 qRT-PCR was performed on the ABI Prism 7900 Sequence Detection System
308 (Applied Biosystems) using SYBR Green. Each set of experiments was repeated three
309 times.

310

311 **Dual-luciferase Reporter Assay System to identify promoter activity**

312 Promoter sequences of 2506 bp and 2984 bp were amplified from W1411 and
313 IRGC104165 genomic DNA, respectively, using the specific pLUCL-F/R primers and
314 transformed into the vector pGreenII0800-LUC using an in-fusion enzyme (Genebank
315 Biosciences) (Hellens et al., 2005) to generate proW1411:LUC and pro
316 IRGC104165:LUC plasmids, respectively. The plasmids were co-infiltrated into rice
317 protoplasts of ZH17. Firefly and Renilla LUC activities were measured using a
318 Dual-luciferase Reporter Assay System (Promega).

319

320 **Methylation-specific PCR**

321 The DNA was treated using a DNA Bisulfite Conversion Kit. Then,
322 methylation-specific PCR was performed using a Methylation-specific PCR Kit. Both
323 kits were purchased from TIANGEN BIOTECH.

324

325 **Subcellular localization.**

326 The *GLAG5* CDs of W1411 without the stop codon was fused to the N-terminus of
327 green fluorescent protein driven by the 35S promoter. The constructed vector was
328 co-infiltrated into rice protoplasts of ZH17 and observed using an Olympus FV1000
329 fluorescence microscope.

330

331 **Primers**

332 The primer sequences used in this research are listed in Table S2.

333

334 **The sequencing data**

335 The next-generation sequencing data of 94 *O. barthii* samples, with the GenBank
336 accession numbers SRR1206362–SRR1206455, were downloaded from the SRA of
337 NCBI, and the sequencing data for the 110 *O. glaberrima* samples, with the GenBank
338 accession numbers SRR3231659–SRR3231748 and SRR1206500–SRR1206519,
339 were also downloaded from the SRA of NCBI (Wang et al., 2014; Meyer et al., 2016).
340 A total of 3,619,010 and 12,004,364 SNPs were identified across the 110 *O.*
341 *glaberrima* accessions and 94 *O. barthii* accessions, respectively, and were used to
342 measure genome-wide levels of π .

343

344 **DNA sequencing data analysis and SNP calling**

345 The DNA re-sequencing data of all the samples were subjected to quality control
346 using Trimomatic (Bolger et al., 2014), and then, the remaining qualified reads were
347 aligned using BWA to the reference sequence, the *Oryza glaberrima* genome
348 (IRGC104165). The alignments were sorted, and duplicate reads were removed using
349 SamTools (<https://www.htslib.org>). Final SNP calling was performed using the
350 Genome Analysis Toolkit (GATK) HaplotypeCaller with the default parameters. For
351 the SNP set from the 204 samples, the filter settings were as follows: DP > 16,200,
352 QD < 2.0, FS > 60.0, MQ < 40.0, SOR > 3.0, MQRankSum < -12.5 and
353 ReadPosRankSum < -8.0.

354

355 **Selection sweeps analyses**

356 Genome-wide π was calculated using VCFtools V0.1.17 for nonoverlapping 100-kb
357 windows and a 1-kb step size across the genomes of *O. glaberrima* and *O. barthii*.
358 Distributions of π and $\pi_{\text{wild}} (\pi_w) / \pi_{\text{cultivated}} (\pi_c)$ ratios within the regions associated with
359 the *hAT* TE were determined. The distribution of π_w / π_c along the chromosome was

360 plotted using an R script.

361

362 **CRedit authorship contribution statement**

363 **Leqin Chang:** Investigation, Validation, Writing - Original draft, Review & Editing.

364 **Min Hu:** Data curation, Investigation. **Jing Ning:** Data curation, Investigation. **Wei**

365 **He:** Data curation, Validation. **Jiayu Gao:** Data curation. **Marie-Noelle Ndjondjop:**

366 Writing - Review & Editing. **Yongcai Fu:** Resources. **Fengxia Liu:** Writing - Review

367 & Editing. **Hongying Sun:** Data curation. **Ping Gu:** Resources. **Chuanqing Sun:**

368 Resources, Supervision. **Zuofeng Zhu:** Conceptualization, Project administration,

369 Resources, Supervision, Writing - Original draft, Review & Editing.

370

371 **Conflict of interest**

372 The authors declare no conflict of interests.

373

374 **Acknowledgments**

375 We thank the International Rice Research Institute, the Japan National Institute of

376 Genetics and the United States Department of Agriculture-Agricultural Research

377 Service for providing the wild rice and cultivated rice samples. This research was

378 supported by the National Natural Science Foundation of China (31925029). The

379 funders had no role in the study design, data collection and analysis, decision to

380 publish or manuscript preparation.

References

- 382 Ammiraju, J.S.S., Lu, F., Sanyal, A., Yu, Y., Song, X., Jiang, N., Pontaroli, A.C.,
383 Rambo, T., Currie, J., Collura, K., Talag, J., Fan, C.Z., Goicoechea, J.L., Zuccolo,
384 A., Chen, J., Bennetzen, J.L., Chen, M.S., Jackson, S., Wing, R.A., 2008.
385 Dynamic Evolution of *Oryza* Genomes Is Revealed by Comparative Genomic
386 Analysis of a Genus-Wide Vertical Data Set. *Plant Cell*. 20, 3191-3209.
- 387 Angeles-Shim, R.B., Asano, K., Takashi, T., Shim, J., Kuroha, T., Ayano, M.,
388 Ashikari, M., 2012. A WUSCHEL-related homeobox 3B gene, *depilous* (*dep*),
389 confers glabrousness of rice leaves and glumes. *Rice* 5, 1-12.
- 390 Atkinson, P.W., Warren, W.D., Obrochta, D.A., 1993. The Hobo Transposable
391 Element of *Drosophila* Can Be Cross-Mobilized in Houseflies and Excises Like
392 the *Ac* Element of Maize. *Proc. Natl. Acad. Sci. U. S. A.* 90, 9693-9697.
- 393 Bolger, A.M., Lohse, M., Usadel, B., 2014. Trimmomatic: a flexible trimmer for
394 Illumina sequence data. *Bioinformatics* 30, 2114-2120.
- 395 Chen, J.F., Huang, Q.F., Gao, D.Y., Wang, J.Y., Lang, Y.S., Liu, T.Y., Li, B., Bai,
396 Z.T., Goicoechea, J.L., Liang, C.Z., Chen, C.B., Zhang, W.L., Sun, S.H., Liao,
397 Y., Zhang, X.M., Yang, L., Song, C.L., Wang, M.J., Shi, J.F., Liu, G., Liu, J.J.,
398 Zhou, H.L., Zhou, W.L., Yu, Q.L., An, N., Chen, Y., Cai, Q., Wang, B., Liu,
399 B.H., Min, J.M., Huang, Y., Wu, H.L., Li, Z.Y., Zhang, Y., Yin, Y., Song, W.Q.,
400 Jiang, J.M., Jackson, S.A., Wing, R.A., Wang, J., Chen, M.S., 2013.
401 Whole-genome sequencing of *Oryza brachyantha* reveals mechanisms
402 underlying *Oryza* genome evolution. *Nat. Commun.* 4, 1595.
- 403 Chen, S.Y., Wang, S.C., 2019. *GLABRA2*, a Common Regulator for Epidermal Cell
404 Fate Determination and Anthocyanin Biosynthesis in *Arabidopsis*. *Int. J. Mol.*
405 *Sci.* 20, 4997.
- 406 Feschotte, C., Jiang, N., Wessler, S.R., 2002. Plant transposable elements: Where
407 genetics meets genomics. *Nat. Rev. Genet.* 3, 329-341.
- 408 Feschotte, C., Pritham, E.J., 2007. DNA transposons and the evolution of eukaryotic
409 genomes. *Annu. Rev. Genet.* 41, 331-368.
- 410 Friedli, M., Trono, D., 2015. The Developmental Control of Transposable Elements
411 and the Evolution of Higher Species. *Annu. Rev. Cell. Dev. Bi.* 31, 429-451.
- 412 Fujino, K., Sekiguchi, H., 2011. Transposition behavior of nonautonomous a hAT
413 superfamily transposon *nDart* in rice (*Oryza sativa* L.). *Mol. Genet. Genomics.*
414 286, 135-142.
- 415 Hellens, R.P., Allan, A.C., Friel, E.N., Bolitho, K., Grafton, K., Templeton, M.D.,
416 Karunairetnam, S., Gleave, A.P., Laing, W.A., 2005. Transient expression
417 vectors for functional genomics, quantification of promoter activity and RNA
418 silencing in plants. *Plant Methods*. 1, 13.
- 419 Hu, M., Lv, S.W., Wu, W.G., Fu, Y.C., Liu, F.X., Wang, B.B., Li, W.G., Gu, P., Cai,
420 H.W., Sun, C.Q., Zhu, Z.F., 2018. The domestication of plant architecture in
421 African rice. *Plant J.* 94, 661-669.
- 422 Huang, C., Sun, H.Y., Xu, D.Y., Chen, Q.Y., Liang, Y.M., Wang, X.F., Xu, G.H.,
423 Tian, J.G., Wang, C.L., Li, D., Wu, L.S., Yang, X.H., Jin, W.W., Doebley, J.F.,

424 Tian, F., 2018. ZmCCT9 enhances maize adaptation to higher latitudes. *Proc.*
425 *Natl. Acad. Sci. U. S. A.* 115, E334-E341.

426 Hudson, A.D., Carpenter, R., Coen, E.S., 1990. Phenotypic Effects of Short-Range
427 and Aberrant Transposition in *Antirrhinum-Majus*. *Plant Mol. Biol.* 14, 835-844.

428 Li, J.J., Yuan, Y.D., Lu, Z.F., Yang, L.S., Gao, R.C., Lu, J.G., Li, J.Y., Xiong, G.S.,
429 2012. Glabrous Rice 1, encoding a homeodomain protein, regulates trichome
430 development in rice. *Rice.* 5, 32.

431 Li, X.K., Guo, K., Zhu, X.B., Chen, P., Li, Y., Xie, G.S., Wang, L.Q., Wang, Y.T.,
432 Persson, S., Peng, L.C., 2017. Domestication of rice has reduced the occurrence
433 of transposable elements within gene coding regions. *Bmc. Genomics.* 18, 55.

434 Lim, H.H., Domala, Z., Joginder, S., Lee, S.H., Lim, C.S., Abubakar, C.M., 1984.
435 Rice Millers Syndrome - a Preliminary-Report. *Brit. J. Ind. Med.* 41, 445-449.

436 Lv, S.W., Wu, W.G., Wang, M.H., Meyer, R.S., Ndjiondjop, M.N., Tan, L.B., Zhou,
437 H.Y., Zhang, J.W., Fu, Y.C., Cai, H.W., Sun, C.Q., Wing, R.A., Zhu, Z.F., 2018.
438 Genetic control of seed shattering during African rice domestication. *Nat. Plants.*
439 4, 331-337.

440 Ma, X., Fan, J., Wu, Y., Zhao, S., Zheng, X., Sun, C., Tan, L., 2020. Whole-genome
441 de novo assemblies reveal extensive structural variations and dynamic
442 organelle-to-nucleus DNA transfers in African and Asian rice. *Plant J.* 104,
443 596-612.

444 Mao, H.D., Wang, H.W., Liu, S.X., Li, Z., Yang, X.H., Yan, J.B., Li, J.S., Tran,
445 L.S.P., Qin, F., 2015. A transposable element in a NAC gene is associated with
446 drought tolerance in maize seedlings. *Nat. Commun.* 6, 8326.

447 Meyer, R.S., Choi, J.Y., Sanches, M., Plessis, A., Flowers, J.M., Amas, J., Dorph, K.,
448 Barretto, A., Gross, B., Fuller, D.Q., Bimpong, I.K., Ndjiondjop, M.N., Hazzouri,
449 K.M., Gregorio, G.B., Purugganan, M.D., 2016. Domestication history and
450 geographical adaptation inferred from a SNP map of African rice. *Nat. Genet.* 48,
451 1083-1088.

452 Molina, J., Sikora, M., Garud, N., Flowers, J.M., Rubinstein, S., Reynolds, A., Huang,
453 P., Jackson, S., Schaal, B.A., Bustamante, C.D., Boyko, A.R., Purugganan, M.D.,
454 2011. Molecular evidence for a single evolutionary origin of domesticated rice.
455 *Proc. Natl. Acad. Sci. U. S. A.* 108, 8351-8356.

456 Peng, Y., Zhang, Y.Y., Gui, Y.J., An, D., Liu, J.Z., Xu, X., Li, Q., Wang, J.M., Wang,
457 W., Shi, C.H., Fan, L.J., Lu, B.R., Deng, Y.W., Teng, S., He, Z.H., 2019.
458 Elimination of a Retrotransposon for Quenching Genome Instability in Modern
459 Rice. *Mol. Plant.* 12, 1395-1407.

460 Purugganan, M.D., 2014. An evolutionary genomic tale of two rice species. *Nat Genet*
461 46, 931-932.

462 Sakai, H., Ikawa, H., Tanaka, T., Numa, H., Minami, H., Fujisawa, M., Shibata, M.,
463 Kurita, K., Kikuta, A., Hamada, M., Kanamori, H., Namiki, N., Wu, J.Z., Itoh, T.,
464 Matsumoto, T., Sasaki, T., 2011. Distinct evolutionary patterns of *Oryza*
465 *glaberrima* deciphered by genome sequencing and comparative analysis. *Plant J.*
466 66, 796-805.

467 Stein, J.C., Yu, Y., Copetti, D., Zwickl, D.J., Zhang, L., Zhang, C.J., Chougule, K.,

468 Gao, D.Y., Iwata, A., Goicoechea, J.L., Wei, S.R., Wang, J., Liao, Y., Wang,
469 M.H., Jacquemin, J., Becker, C., Kudrna, D., Zhang, J.W., Londono, C.E.M.,
470 Song, X., Lee, S., Sanchez, P., Zuccolo, A., Ammiraju, J.S.S., Talag, J.,
471 Danowitz, A., Rivera, L.F., Gschwend, A.R., Noutsos, C., Wu, C.C., Kao, S.M.,
472 Zeng, J.W., Wei, F.J., Zhao, Q., Feng, Q., El Baidouri, M., Carpentier, M.C.,
473 Lasserre, E., Cooke, R., Farias, D.D., da Maia, L.C., dos Santos, R.S., Nyberg,
474 K.G., McNally, K.L., Mauleon, R., Alexandrov, N., Schmutz, J., Flowers, D.,
475 Fan, C.Z., Weigel, D., Jena, K.K., Wicker, T., Chen, M.S., Han, B., Henry, R.,
476 Hsing, Y.I.C., Kurata, N., de Oliveira, A.C., Panaud, O., Jackson, S.A., Machado,
477 C.A., Sanderson, M.J., Long, M.Y., Ware, D., Wing, R.A., 2018. Genomes of 13
478 domesticated and wild rice relatives highlight genetic conservation, turnover and
479 innovation across the genus *Oryza* (vol 50, pg 285, 2018). *Nat. Genet.* 50,
480 1618-1618.

481 Studer, A., Zhao, Q., Ross-Ibarra, J., Doebley, J., 2011. Identification of a functional
482 transposon insertion in the maize domestication gene *tb1*. *Nat. Genet.* 43,
483 1160-U1164.

484 Sun, W.Q., Gao, D.W., Xiong, Y., Tang, X.X., Xiao, X.F., Wang, C.R., Yu, S.B.,
485 2017. Hairy Leaf 6, an AP2/ERF Transcription Factor, Interacts with OsWOX3B
486 and Regulates Trichome Formation in Rice. *Mol. Plant.* 10, 1417-1433.

487 Van Andel, T., 2010. African Rice (*Oryza glaberrima* Steud.): Lost Crop of the
488 Enslaved Africans Discovered in Suriname(1). *Econ. Bot.* 64, 1-10.

489 Wang, M.H., Yu, Y., Haberer, G., Marri, P.R., Fan, C.Z., Goicoechea, J.L., Zuccolo,
490 A., Song, X., Kudrna, D., Ammiraju, J.S.S., Cossu, R.M., Maldonado, C., Chen,
491 J., Lee, S., Sisneros, N., de Baynast, K., Golser, W., Wissotski, M., Kim, W.,
492 Sanchez, P., Ndjioudjop, M.N., Sanni, K., Long, M.Y., Carney, J., Panaud, O.,
493 Wicker, T., Machado, C.A., Chen, M.S., Mayer, K.F.X., Rounsley, S., Wing,
494 R.A., 2014. The genome sequence of African rice (*Oryza glaberrima*) and
495 evidence for independent domestication. *Nat. Genet.* 46, 982-988.

496 Wang, Y.L., Nie, J.T., Chen, H.M., Guo, C.L., Pan, J., He, H.L., Pan, J.S., Cai, R.,
497 2016. Identification and mapping of *Tril*, a homeodomain-leucine zipper gene
498 involved in multicellular trichome initiation in *Cucumis sativus*. *Theor. Appl.*
499 *Genet.* 129, 305-316.

500 Wu, W.G., Liu, X.Y., Wang, M.H., Meyer, R.S., Luo, X.J., Ndjioudjop, M.N., Tan,
501 L.B., Zhang, J.W., Wu, J.Z., Cai, H.W., Sun, C.Q., Wang, X.K., Wing, R.A.,
502 Zhu, Z.F., 2017. A single-nucleotide polymorphism causes smaller grain size and
503 loss of seed shattering during African rice domestication. *Nat. Plants.* 3, 17064.

504 Yang, C.X., Li, H.X., Zhang, J.H., Luo, Z.D., Gong, P.J., Zhang, C.J., Li, J.H., Wang,
505 T.T., Zhang, Y.Y., Lu, Y.E., Ye, Z.B., 2011. A regulatory gene induces trichome
506 formation and embryo lethality in tomato. *Proc. Natl. Acad. Sci. U. S. A.* 108,
507 11836-11841.

508 Yang, Q., Li, Z., Li, W.Q., Ku, L.X., Wang, C., Ye, J.R., Li, K., Yang, N., Li, Y.P.,
509 Zhong, T., Li, J.S., Chen, Y.H., Yan, J.B., Yang, X.H., Xu, M.L., 2013.
510 CACTA-like transposable element in *ZmCCT* attenuated photoperiod sensitivity
511 and accelerated the postdomestication spread of maize. *Proc. Natl. Acad. Sci. U.*

512 S. A. 110, 16969-16974.
513 Zhang, H.L., Wu, K., Wang, Y.F., Peng, Y., Hu, F.Y., Wen, L., Han, B., Qian, Q.,
514 Teng, S., 2012. A WUSCHEL-like homeobox gene, OsWOX3B responses to
515 NUDA/GL-1 locus in rice. *Rice* 5, 30.
516 Zhang, X., Zong, J., Liu, J.H., Yin, J.Y., Zhang, D.B., 2010. Genome-Wide Analysis
517 of WOX Gene Family in Rice, Sorghum, Maize, Arabidopsis and Poplar. *J Integr*
518 *Plant Biol* 52, 1016-1026.

519

520

521 **Figure Legends**

522

523 **Fig. 1.** A phenotypic comparison of wild rice W1411 (*O. barthii*) and cultivated rice
524 IRGC104165 (*O. glaberrima*). **A** and **B**: Stereomicroscope images of the seeds of
525 W1411 and IRGC104165. **C–F**: SEM images of the seeds of W1411 and
526 IRGC104165, Scale bars, 24 mm (**A** and **B**); 200 μ m (**C** and **D**); 1 mm (**E** and **F**).

527

528 **Fig. 2.** Map-based cloning of *GLAG5*. **A**: The target gene was mapped to the interval
529 between C03 and RM593 on the short arm of chromosome 5. *GLAG5* was finally fine
530 mapped to an interval approximately 15.9-kb between C02 and C06. **B**: The
531 construction of the complementary vector: a 4.04-kb DNA fragment containing the
532 entire *GLAG5* gene region from the W1411 genome was inserted into the binary
533 vector pCAMIA1300 to generate the complementary transformation vector p*GLAG5*.
534 **C–H**: The phenotypes of a control plant WK21 and transgenic plant (p*GLAG5*)
535 harboring the complementary transformation vector p*GLAG5*. Stereomicroscope
536 images of the seeds of WK21 and p*GLAG5* (**C** and **D**). SEM images of the seeds (**E**
537 and **F**) and leaves of WK21 and p*GLAG5* (**G** and **H**), respectively. Scale bars, 20 mm
538 (**C** and **D**); 800 μ m (**E** and **F**); 7 mm (**G** and **H**).

539

540 **Fig. 3.** The phenotype of gene-editing plant CAS9-*GLAG5*. **A** and **B**:
541 Stereomicroscope images of the seeds of W1411 and gene-editing plant
542 CAS9-*GLAG5*, 20 mm (**A** and **B**); **C** and **D**: SEM images of the seeds of W1411 and
543 CAS9-*GLAG5*, 800 μ m (**C** and **D**); **E** and **F**: SEM images of the leaves of W1411 and
544 CAS9-*GLAG5*, 7 mm (**E** and **F**); **G** and **H**: The auricles (direction of arrow) of
545 W1411 and CAS9-*GLAG5*, 6 mm (**G** and **H**); **I** and **J**: The glumes of W1411 and
546 CAS9-*GLAG5*, 30 mm (**I** and **J**); (**K**) Plant architecture of W1411 and CAS9-*GLAG5*,
547 18 cm (**K**).

548

549 **Fig. 4.** A transposon in the promoter of *GLAG5* led to glabrous glumes in *O*.

550 *glaberrima*. **A:** Sequence analysis of the *hAT* transposon. **B:** Tissue expression of
551 *GLAG5*. The expression of *GLAG5* was detected in root, stem, leaf, leaf sheath and
552 young panicle. Values are means \pm SDs ($n = 3$). **, $P < 0.01$; *, $0.01 < P < 0.05$,
553 (two-tailed Student's *t*-test). **C:** Dual-LUC reporter assays showing that the promoter
554 activities of *GLAG5* from W1411 and IRGC104165 were affected differently by the
555 *hAT* transposon. Values are means \pm SDs ($n = 4$). **, $P < 0.01$, (two-tailed Student's
556 *t*-test). **D:** Methylation-specific PCR. SD, standard deviation.

557

558 **Fig. 5.** Evidence of positive selection on the *GLAG5* gene region in *O. glaberrima*. **A:**
559 Proportion of glabrous glumes in wild rice *O. barthii*. **B:** Proportion of glabrous
560 glumes in African cultivated rice *O. glaberrima*. **C:** Distribution of nucleotide
561 diversity (π) and $\pi_{\text{wild}} (\pi_w)/\pi_{\text{cultivated}} (\pi_c)$ ratios within the regions associated with the
562 *hAT* transposon. The π levels within a 100-kb sliding window with a 1-kb step size in
563 *O. glaberrima* and *O. barthii*. The translucent orange bars at the bottom represent
564 selective sweeps.

565

Fig 1

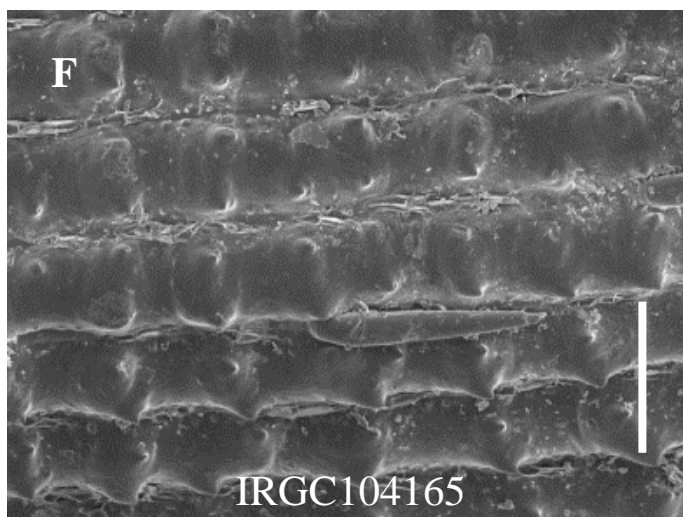
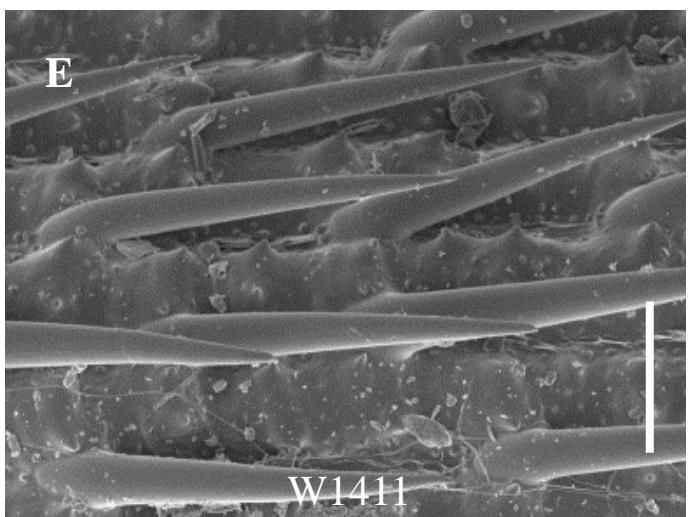
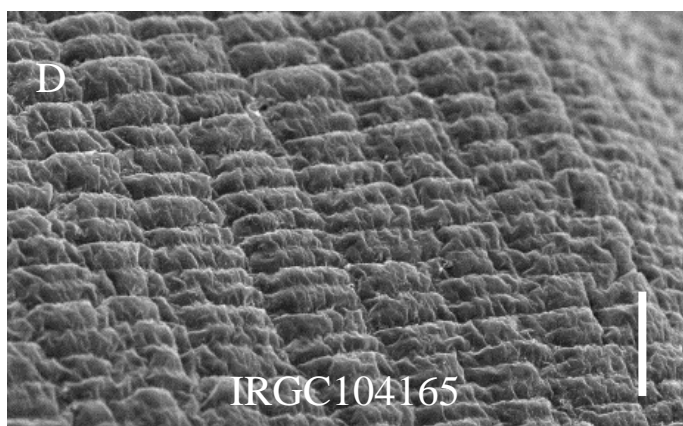
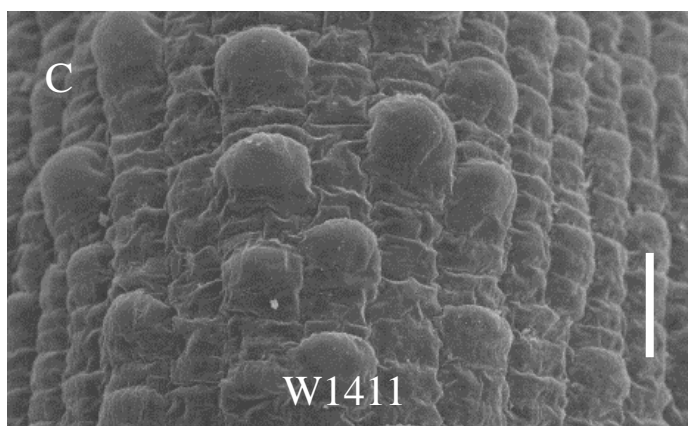


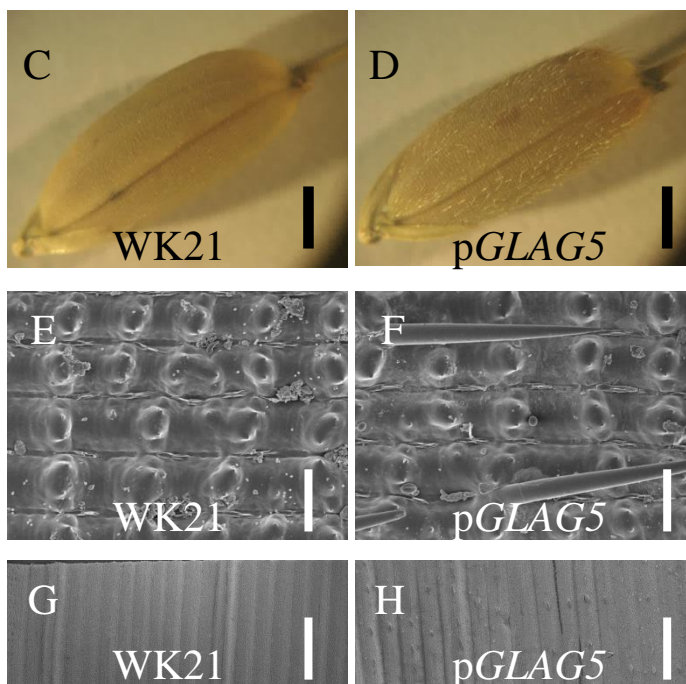
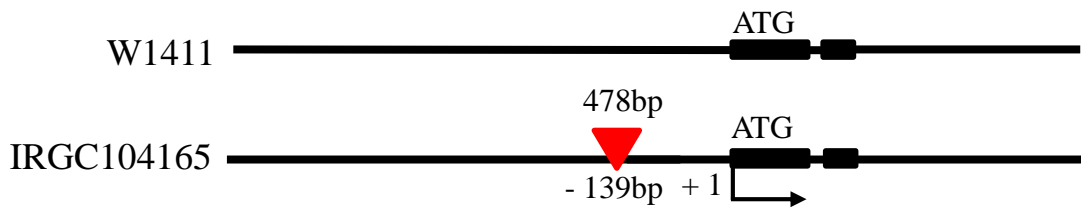
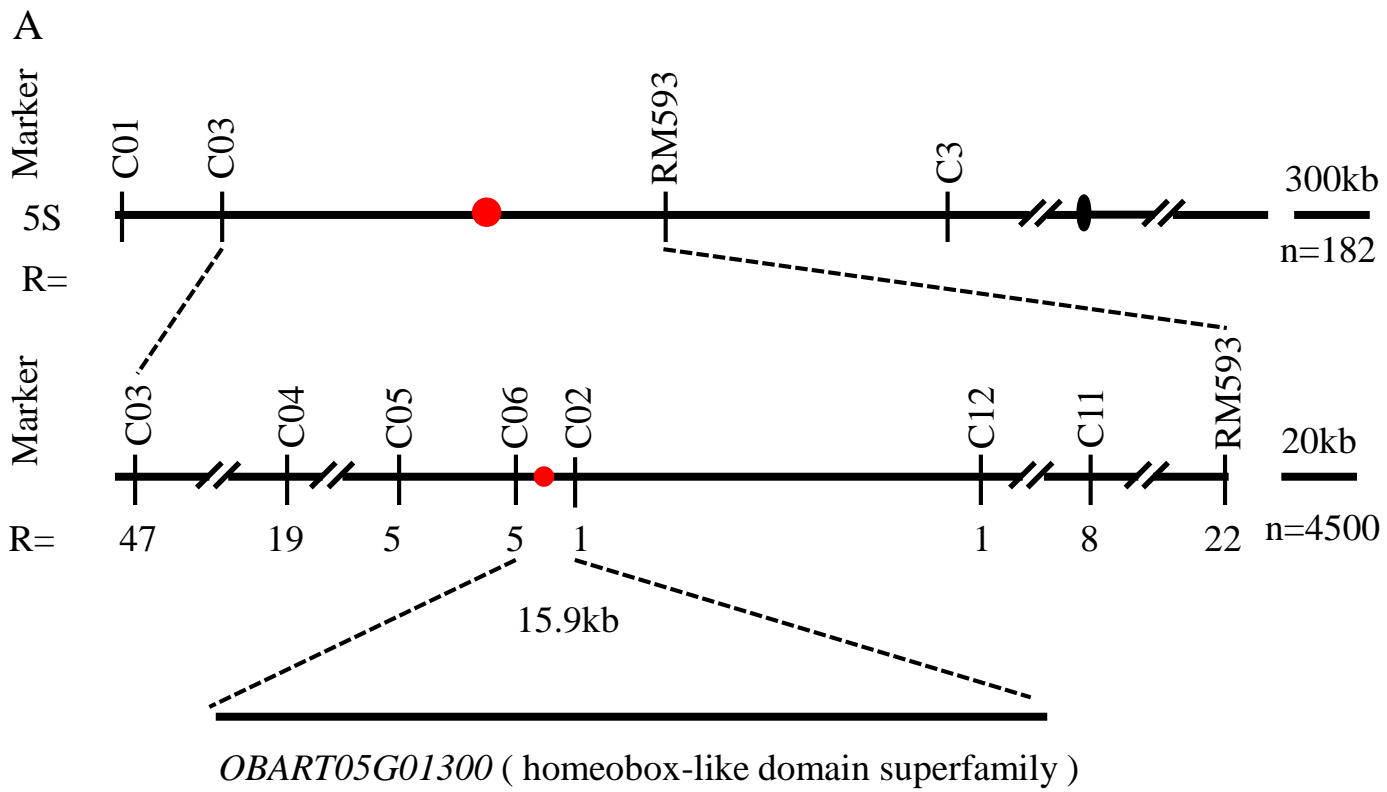
Fig 2

Fig 3

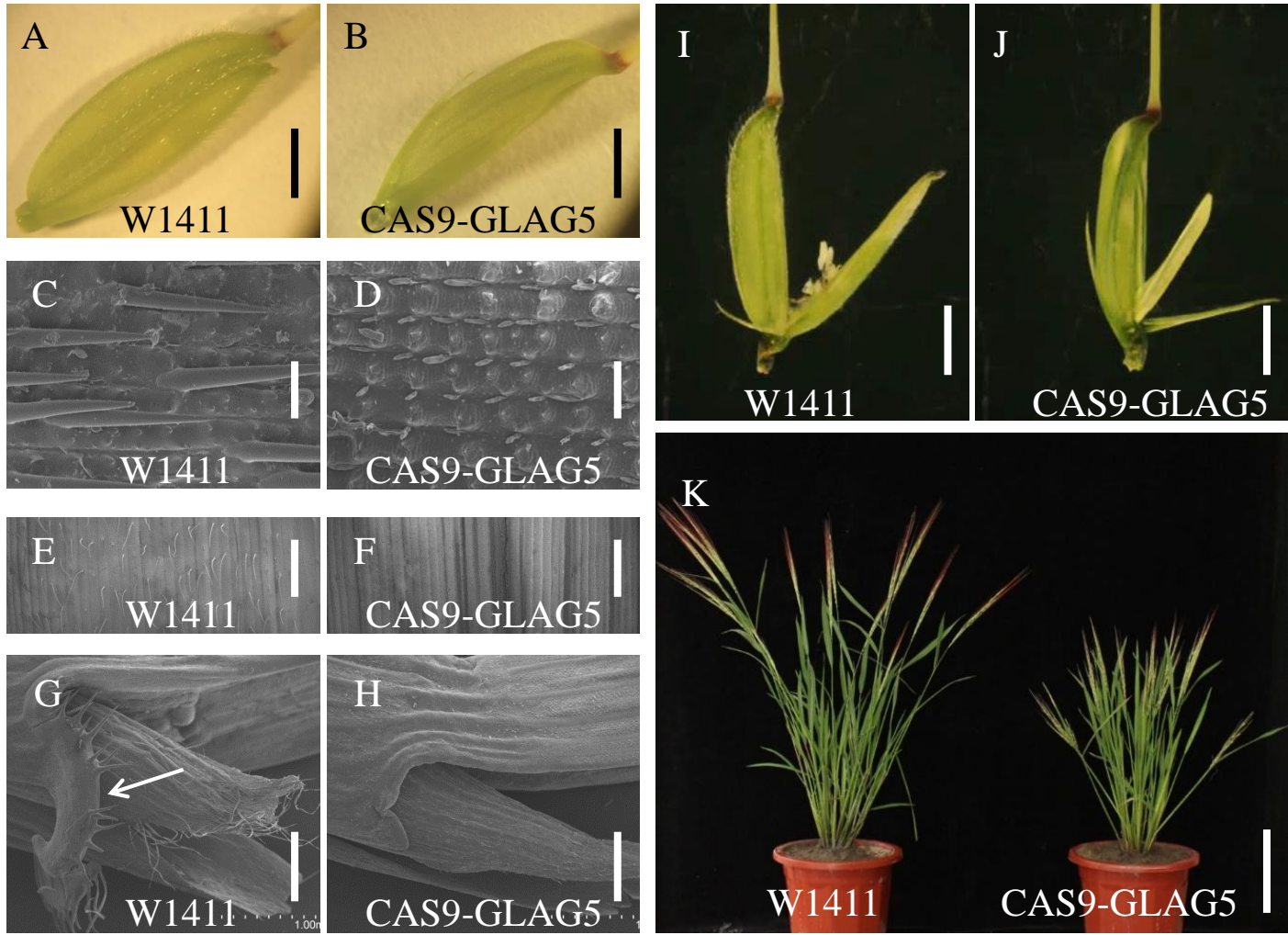
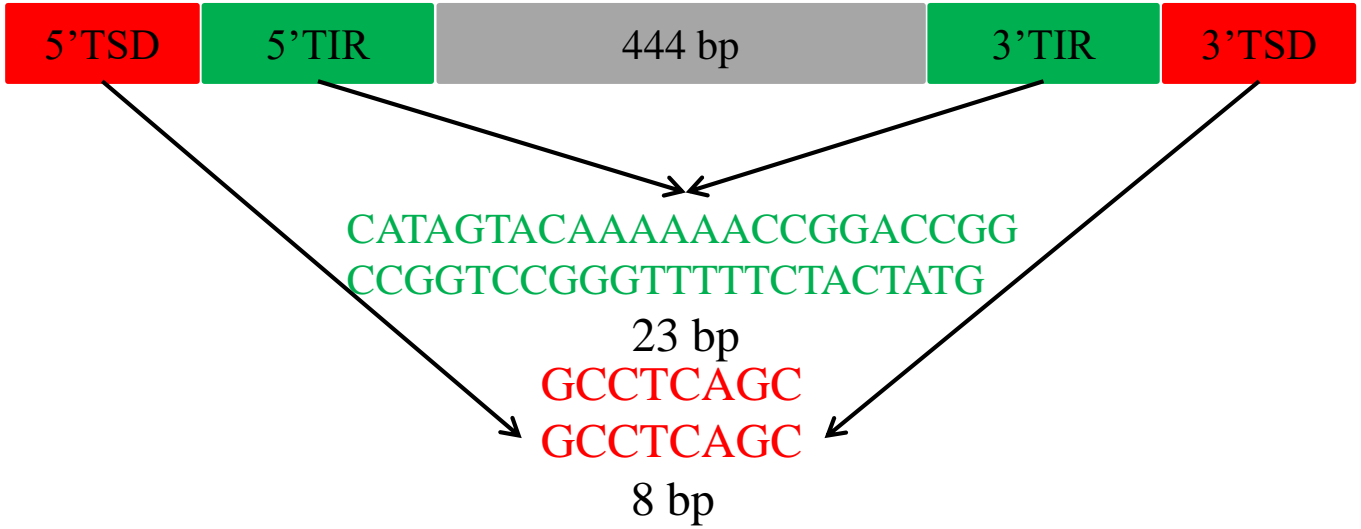


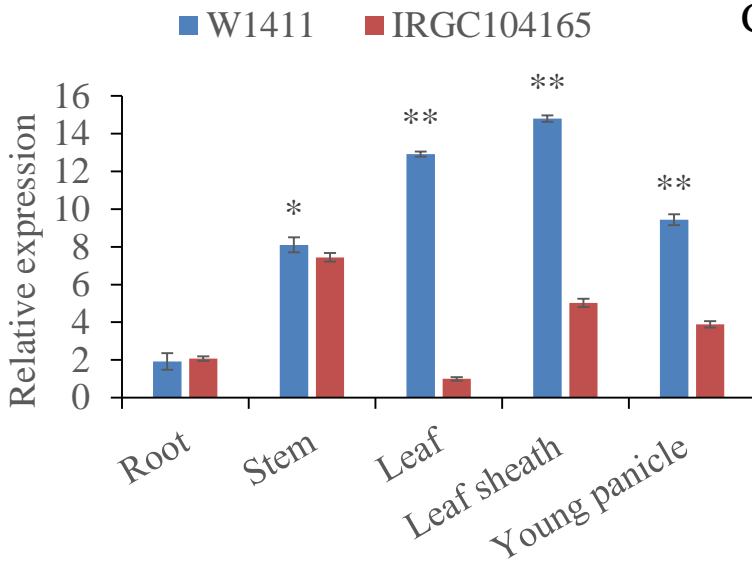
Fig 4

A

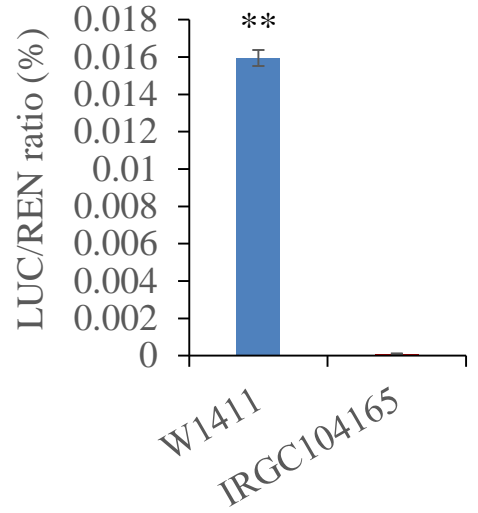
The *hAT* transposons



B



C



D

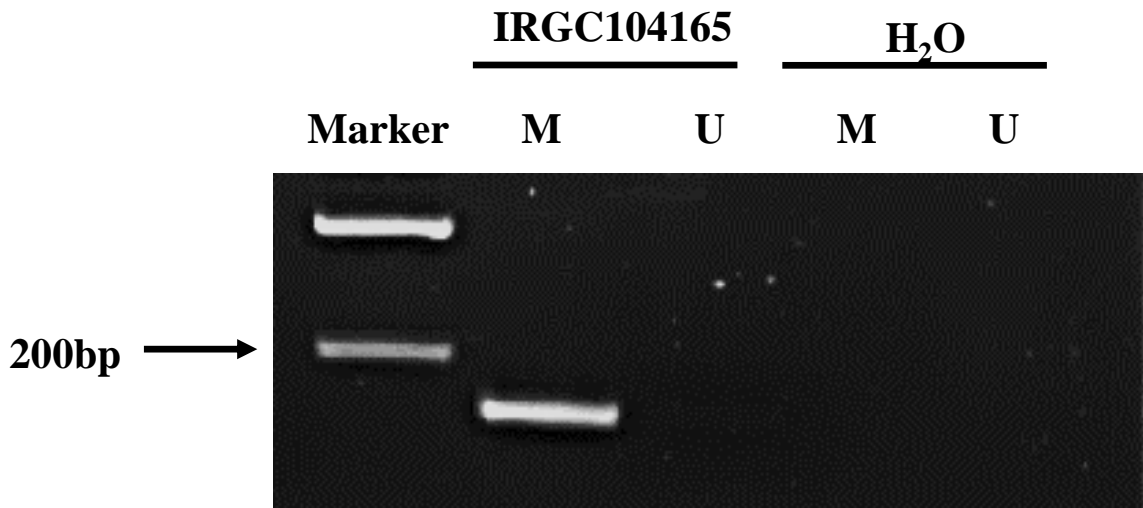
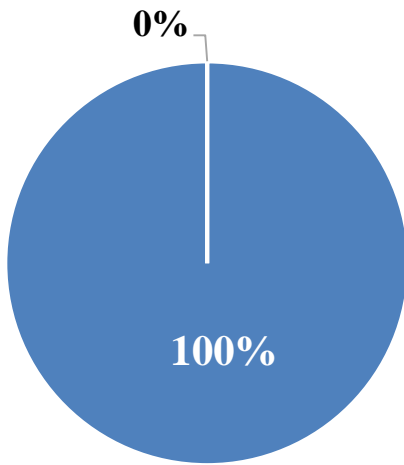


Fig 5

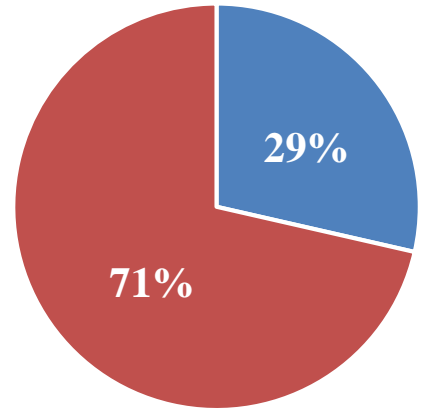
A



■ Trichomes ■ Glabrous Rice

O. barthii

B



■ Trichomes ■ Glabrous rice

O. glaberrima

C

